

ACCEPTED MANUSCRIPT

Osteogenic effects of simvastatin-loaded mesoporous titania thin films

To cite this article before publication: Miriam Lopez-Alvarez *et al* 2017 *Biomed. Mater.* in press <https://doi.org/10.1088/1748-605X/aa95f1>

Manuscript version: Accepted Manuscript

Accepted Manuscript is “the version of the article accepted for publication including all changes made as a result of the peer review process, and which may also include the addition to the article by IOP Publishing of a header, an article ID, a cover sheet and/or an ‘Accepted Manuscript’ watermark, but excluding any other editing, typesetting or other changes made by IOP Publishing and/or its licensors”

This Accepted Manuscript is © 2017 IOP Publishing Ltd.

During the embargo period (the 12 month period from the publication of the Version of Record of this article), the Accepted Manuscript is fully protected by copyright and cannot be reused or reposted elsewhere.

As the Version of Record of this article is going to be / has been published on a subscription basis, this Accepted Manuscript is available for reuse under a CC BY-NC-ND 3.0 licence after the 12 month embargo period.

After the embargo period, everyone is permitted to use copy and redistribute this article for non-commercial purposes only, provided that they adhere to all the terms of the licence <https://creativecommons.org/licenses/by-nc-nd/3.0>

Although reasonable endeavours have been taken to obtain all necessary permissions from third parties to include their copyrighted content within this article, their full citation and copyright line may not be present in this Accepted Manuscript version. Before using any content from this article, please refer to the Version of Record on IOPscience once published for full citation and copyright details, as permissions will likely be required. All third party content is fully copyright protected, unless specifically stated otherwise in the figure caption in the Version of Record.

View the [article online](#) for updates and enhancements.

Osteogenic effects of simvastatin-loaded mesoporous titania thin films

Miriam López-Álvarez^{1*}, Vanesa López-Puente², Cosme Rodríguez-Valencia¹,
Paula C. Angelomé³, Luis M. Liz-Marzán^{4,5,6}, Julia Serra¹, Isabel Pastoriza-
Santos², Pío González¹

¹New Materials Group, Applied Physics Dpt, IISGS, University of Vigo, Spain

²Departamento de Química-Física, CINBIO, Universidade de Vigo, 36310, Spain

³Gerencia Química, Centro Atómico Constituyentes, Comisión Nacional de
Energía Atómica, CONICET, Av. Gral Paz 1499, B1650KNA, San Martín,
Buenos Aires, Argentina

⁴CIC biomaGUNE, Paseo de Miramón 182, 20014 Donostia-San Sebastián, Spain

⁵Ikerbasque Basque Foundation for Science, 48013 Bilbao, Spain

⁶CIBER de Bioingeniería, Biomateriales y Nanomedicina, CIBER-BBN, 20014
Donostia-San Sebastián, Spain

E-mail addresses: miriammsd@uvigo.es, vanelope@uvigo.es, cosme@uvigo.es,
angelome@cnea.gov.ar, llizmarzan@cicbiomagune.es, jserra@uvigo.es,
pastoriza@uvigo.es, pglez@uvigo.es

Corresponding author: Miriam López Álvarez, New Materials Group, Applied
Physics Dpt., School of Industrial Engineering, Campus Lagoas-Marcosende,
University of Vigo, 36310, Spain

E-mail: miriammsd@uvigo.es

Telephone: +34 986130158 // Fax: +34 986812201

Running head: Simvastatin-loaded mesoporous titania thin films

Abstract

The use of statins in the field of bone regeneration is under current investigation due to the existing demand for non-toxic anabolic agents capable of enhancing bone formation in cases of substantial loss. Simvastatin, a coenzyme currently prescribed in clinics to inhibit cholesterol biosynthesis, has been proven to promote osteogenic differentiation by stimulating bone formation and inhibiting osteoclasts activity. We present the loading of simvastatin in mesoporous TiO₂ thin films toward combining the pro-osteogenic properties of this molecule with the demonstrated bioactivity of titania. TiO₂ thin films processing and characterization were carried out, as well as evaluation of MC3T3-E1 pre-osteoblasts viability when directly incubated with different concentrations of simvastatin, followed by the analysis of osteogenic activity promoted by simvastatin upon loading in the thin films. The accessible porosity of 36 % quantified on the 95±5 nm thick mesoporous thin films, together with pore diameters of 5.5 nm, necks between pores of 2.8 nm and interpore distances of 12±2 nm allow the loading of the simvastatin molecule, as confirmed by FTIR spectroscopy. Simvastatin was found to promote MC3T3-E1 pre-osteoblasts viability at concentrations ≤ 0.01 g/L, with a cytotoxicity threshold of 0.05 g/L. We additionally found that film loadings with 0.001 g/L simvastatin promotes statistically higher MC3T3-E1 pre-osteoblast proliferation whereas a higher concentration of 0.01 g/L leads to statistically higher osteogenic activity (ALP synthesis), after 21 days of incubation, as compared to unloaded films. These results demonstrate the potential of simvastatin local administration based on bioactive mesoporous thin films to promote pro-osteogenic properties. By focusing this strategy on the coating of metallic prostheses, the supply of simvastatin to the target tissue can be favored and risks of systemic side effects will be reduced while enhancing the osteointegration of the implants.

Keywords: simvastatin, mesoporous titania, thin films, osteogenic activity, drug delivery.

1. Introduction

The main strategy in clinics to restore functionality in cases of critically damaged bone tissue, such as in osteoporosis (Kanis *et al* 2013) or periodontal diseases (Sayar *et al* 2016), comprises its replacement by metallic alloys. These metallic implants (such as Ti₆Al₄V alloy) present

1
2
3 appropriate mechanical properties and biocompatibility. However, limitations in terms of
4
5 bioactivity and osteointegration are commonly experienced, which give rise to problems at
6
7 implant fixation, apart from infection and inflammation cases after the implant surgery (Xia *et*
8
9 *al* 2012). Thus, to increase the bioactivity and osteointegration of these implants, cell-
10
11 biomaterial interactions must be improved. These interactions have been demonstrated to be
12
13 highly influenced by the stiffness, topography and chemical composition of the implant surface
14
15 (Bellino *et al* 2013). Bioactive materials favor direct surface formation of apatite *in vivo*, which
16
17 subsequently enables bone bonding (Karlsson *et al* 2015a). Among the wide variety of bioactive
18
19 materials, titania is considered as a highly suitable biocompatible material for bone-anchoring
20
21 implants exhibiting little or no toxicity, both *in vitro* and *in vivo* (Gertler *et al* 2010).
22
23

24
25 Moreover, these ceramics can be deposited as thin films over metallic alloys to provide the cells
26
27 with a bioactive surface. Evaporation-induced self-assembly (EISA) is a very versatile chemical
28
29 methodology (Brinker *et al* 1999) by which mesoporous titania thin films can be easily obtained
30
31 onto a wide variety of substrates with a tunable mesoscopic topography and controlled
32
33 wettability, porosity and chemical properties, based on a combination of sol gel chemistry,
34
35 supramolecular templates and surface modifications (Soler-Illia *et al* 2012, Sanchez *et al* 2008).
36
37 These mesoporous titania thin films have been proven to promote *in vivo* enhanced initial bone
38
39 contact and improved distribution of bone tissue. This is due to the highly ordered arrays of
40
41 monodisperse pores, high specific surface areas and bioactive properties (Meretoja *et al* 2007),
42
43 which influence and eventually lead to the control of osteoblast adhesion and proliferation. The
44
45 improvement of the initial attachment of cells onto the implant surfaces promotes enhanced
46
47 integration of the implant and longer term stability (Bellino *et al* 2013).
48
49

50
51 Mesoporous materials have additionally shown great potential in drug delivery applications to
52
53 provide and maintain drug concentrations within the therapeutic window for the desired period
54
55 of time. The unique features of mesoporous biomaterials, such as high specific surface area, and
56
57 tunable pore-size (with pore diameters between 2 and 50 nm), -volume and -symmetry (ordered
58
59 distribution), allow drug release to occur in a highly reproducible and predictable manner
60
(Karlsson *et al* 2015a). This is of great interest since it is believed that the local drug loading of

1
2
3 antibiotics, anti-inflammatory medicines and growth factors, commonly prescribed orally,
4
5 intravenously, intramuscularly or topically after the implant surgery, contributes to enhancing
6
7 the efficiency of these drugs, while the classic systemic routes hinder them from reaching the
8
9 interface of implants and tissues (Xia *et al* 2012). The controlled local delivery of drugs at the
10
11 implant might bring an efficient therapeutic treatment, since it would administrate the drug
12
13 directly at the targeted cells for a prolonged time period, and thus reduce the risk of systemic
14
15 side effects (Karlsson *et al* 2015a).
16
17

18
19 In the specific case of bone-anchoring implants, it has been demonstrated that their
20
21 osseointegration capacity can be improved by using an inbuilt drug delivery system, such as
22
23 modified mesoporous composites and mesoporous bioactive glasses, which can locally
24
25 administer drugs. For instance, Karlsson *et al* (2015b) proved that the local loading of the
26
27 osteoporosis bisphosphonate drug alendronate, clinically used by oral administration, promoted
28
29 more extensive bone formation. Different antibiotics were also loaded at hosting molecules for
30
31 efficient prevention of infections, as demonstrated by Xia *et al* (2012) by loading cephalothin in
32
33 titanium dioxide coatings. Anti-inflammatory drugs (ibuprofen) were also tested by McMaster
34
35 *et al* (2012) in collagen-templated bioactive titanium dioxide porous networks.
36
37

38
39 Simvastatin, a hydroxy-3-methylglutaryl coenzyme A (HMG-CoA) reductase inhibitor, is
40
41 known to inhibit cholesterol biosynthesis and is currently clinically prescribed for that purpose.
42
43 Several recent studies have demonstrated that this cholesterol-lowering drug also promotes
44
45 osteogenic differentiation, stimulating bone formation *in vitro* and *in vivo* (Maeda *et al* 2001,
46
47 Mundy *et al* 1999, Yin *et al* 2012). The mechanism is thought to be related with the promotion
48
49 of mitochondrial function (cell proliferation) and stimulation of the expression of the bone
50
51 morphogenic protein-2 (BMP-2), a growth factor involved in osteoblast activation. In addition,
52
53 simvastatin seems to participate in osteoclast inhibition by stimulating neovascularization
54
55 (increasing the secretion of vascular endothelial growth factor) (Kheirallah and Almeshaly
56
57 2016).
58

59
60 The topical administration of simvastatin has been proposed to improve the pro-angiogenic and
pro-osteogenic properties of bioglass putty in rat calvaria critical-size defects without significant

1
2
3 inflammation, stimulating BMP-2 and VEGF mRNA expression in osteoblasts (Allon *et al*
4
5 2012) compared to bioglass without topical simvastatin up to 4 weeks of implantation. The
6
7 effects of simvastatin on osteoblastic differentiation *in vitro* were evaluated by Maeda *et al*
8
9 (2001) to demonstrate that simvastatin enhances alkaline phosphatase (ALP) activity and
10
11 mineralization in a dose- and time-dependent fashion. Mundy *et al* (1999) injected simvastatin
12
13 (together with lovastatin) subcutaneously in calvaria of mice, resulting in increased bone
14
15 formation; moreover when simvastatin was orally administered in rats, increased cancellous
16
17 bone volume was also quantified. The use of statins is of great current interest as there is a clear
18
19 need for non-toxic anabolic agents that will substantially increase bone formation in people who
20
21 have already suffered substantial bone loss (Mundy *et al* 1999).
22
23

24
25 However, the systemic administration of statins has been related to serious side effects that can
26
27 be avoided by means of local delivery of the molecule. Moreover, clinical studies suggest that
28
29 orally administered statins may be degraded in the liver, so little of the drug is available to
30
31 accumulate in bone. If higher doses of systemic applied simvastatin are provided, the risk of
32
33 liver failure, kidney disease, rhabdomyolysis, myalgia and other side effects increase as well
34
35 (Kheirallah and Almeshaly 2016). Therefore TiO₂-based biomaterials loaded with simvastatin
36
37 present good prospect as coatings of metallic implants that can provide a combination of local
38
39 drug delivery and bioactivity (direct bone-bonding capability) to be used for biomedical
40
41 applications, such as treatment and regeneration of bone defects.
42
43

44
45 These small molecules that activate the promoter of the bone morphogenetic protein-2 gene can
46
47 be readily loaded into the meso-porosity of titania thin films to provide metallic prosthesis with
48
49 higher osteointegration (due to the bioactivity of the titania film) and with pro-osteogenic
50
51 properties (due to local simvastatin loading), thereby promoting increased expression of the
52
53 bone morphogenetic protein-2 (BMP-2) gene in bone cells. The processing and characterization
54
55 of TiO₂ mesoporous coatings, their loading with different concentrations of simvastatin as well
56
57 as the biological response in terms of proliferation and osteogenic activity of MC3T3-E1 pre-
58
59 osteoblasts are the main objectives of the present work.
60

2. Materials and Methods

2.1 Mesoporous thin films

Glass discs (6 mm in diameter, Thermo Scientific) were sonicated in ethanol for 30 min and then copiously rinsed with Milli-Q water and stored in water until use. Titania mesoporous thin films were fabricated on the glass disc surfaces through the EISA approach as previously reported (Crepaldi *et al* 2003). Briefly, a precursor mixture of TiCl_4 (Aldrich), Pluronic F127 ($(\text{HO}(\text{CH}_2\text{CH}_2\text{O})_{106}(\text{CH}_2\text{CH}(\text{CH}_3)\text{O})_{70}(\text{CH}_2\text{CH}_2\text{O})_{106}\text{OH})$, Sigma), EtOH (pure grade, ACS) and Milli-Q water was prepared. $\text{TiCl}_4/\text{EtOH}/\text{F127}/\text{H}_2\text{O}$ mixtures presented a 1:40:0.005:10 molar ratio of the reagents. Then, 125 μL of the freshly prepared mixture was spin-coated (4000 rpm) on top of the glass discs. The deposited films were then placed in 50 % relative humidity chambers (obtained with a NaBr saturated solution in water) for 24 h and subjected to a stabilizing thermal treatment comprising two successive 24 h heating steps at 60 °C and 120 °C and a final step at 200 °C for 2 h. The F127, acting as template, was finally removed by immersing the films in ethanol for 3 days.

2.2 Physicochemical characterization

Transmission electron microscopy (TEM) images were obtained with a JEOL JEM 1010 microscope operating at an accelerating voltage of 100 kV. Samples for TEM were obtained by scratching the films from the substrate and depositing them on carbon- and FORMVAR-coated copper grids. Scanning electron microscopy (SEM) images from the top and the cross section of the films were obtained with a JEOL JSM-6700 FEG scanning electron microscope operating at an accelerating voltage of 10 kV.

The porosity and pore size distribution were assessed by Environmental Ellipsometric Porosimetry with a SE SOPRA GES-5 spectroscopic ellipsometer in microspot configuration. This technique consists of performing spectroscopic ellipsometry measurements while varying water vapor pressure in a controlled humidity chamber. From those measurements, refractive index variation as a function of humidity is obtained and total accessible volume is calculated by using a Lorentz-Lorenz effective medium approximation. The size distribution of pores and

1
2
3 necks was determined from the adsorption and desorption branches of the isotherms, through
4 the Kelvin equation, taking into account the water contact angle of the sample. The data were
5 analyzed with Winelli software (Boissiere *et al* 2005, Soler-Illia *et al* 2012).
6
7

8
9 Raman spectra were collected using a Renishaw InVia Reflex system. The spectrograph uses
10 high resolution grating (1200 cm^{-1}) with additional band-pass filter optics, a confocal
11 microscope and a 2D-CCD camera. All measurements were made in a confocal microscope in
12 backscattering geometry using a 20X objective with accumulation times of 10 s and a excitation
13 laser line of 532 nm (Nd:YAG).
14
15
16
17
18
19

20 Fourier transform infrared (FTIR) spectra were recorded in Transmission mode using a Nicolet
21 5PCFT-IR spectrometer in the $4000\text{--}400\text{ cm}^{-1}$ range. Samples were prepared by scratching the
22 film and mixing it with KBr, to form a pellet.
23
24
25
26
27

28 *2.3 Determination of cytotoxicity threshold and loading of simvastatin*

29
30 The cytotoxicity threshold was first determined in order to select the optimal simvastatin
31 concentrations to be tested. Direct cell seeding of the MC3T3-E1 pre-osteoblasts (ECACC, UK)
32 with a wide range of simvastatin ($\text{C}_{25}\text{H}_{38}\text{O}_5$, Sigma S6196, >97 % purity) concentrations in
33 ethanol (5; 1; 0.5; 0.1; 0.05; 0.01; 0.001; 0 g/L) was carried out up to 4 days of incubation.
34
35 Thus, 20 μL aliquots from each concentration were added to the corresponding well (96 well
36 microplate) and once ethanol was evaporated, 100 μL of cell suspension ($1.7 \times 10^5\text{ cel/mL}$) in
37 supplemented MEM-alpha medium (Lonza BE02-002F) were added. After 4 days of incubation,
38 and without medium refreshment to maintain the simvastatin concentrations, cell proliferation
39 was quantified with the Cell Proliferation Kit I (MTT assay, Roche), based on the reduction of
40 the yellow tetrazolium salt MTT (3-(4,5-dimethylthiazolyl-2)-2,5-diphenyl tetrazolium bromide)
41 into insoluble purple formazan crystals by the mitochondrial enzyme succinate dehydrogenase,
42 only present in living cells. To this end, 10 μL of MTT labeling reagent in phosphate buffered
43 saline (PBS) was added to each well for 4 hours ($37\text{ }^\circ\text{C}$, 5 % CO_2). Formazan crystals were
44 subsequently solubilized with 100 μL of 10% sodium dodecyl sulfate (SDS) in 0.01 M HCl.
45
46
47
48
49
50
51
52
53
54
55
56
57
58
59
60 The plate was incubated overnight and the resulting colored solution was quantified at 595 and

655 nm using a Bio-Rad Model 550 microplate spectrophotometer. Four replicates per condition were evaluated.

The mesoporous TiO₂ thin films deposited on glass substrates were then sterilized by immersion in 70 % ethanol for 48 h at 2-8 °C. After that, ethanol was removed and samples dried in a laminar flow chamber. The loading of TiO₂ thin films with simvastatin was performed by addition (discs already placed in 96-well microplates) of 20 µL of simvastatin solution in ethanol and maintained for 48 h at 2-8 °C. Different simvastatin concentrations, 0.01 g/L, 0.001 g/L and 0 g/L (reference material), were tested. Finally, the samples were dried in the laminar flow chamber before cell seeding. Simvastatin loaded thin films with a concentration of 5 g/L were also characterized by using a Nicolet 5PCFT-IR spectrophotometer in the 4000–400 cm⁻¹ range. Samples were prepared by scratching the film and mixing it with KBr, to form a pellet.

2.4 Biological response of simvastatin-loaded mesoporous thin films

A concentration of 1.7×10^5 cells/mL of MC3T3-E1 pre-osteoblasts in 100 µL of MEM-alpha supplemented with 10 % Fetal Bovine Serum (FBS; Lonza DE14-801E) and 1 % Antibiotic Antimycotic Solution with 10000 units of penicillin, 10 mg of streptomycin and 25 µg of amphotericin B per mL (Sigma A5955) were seeded on the TiO₂ + 0.01, TiO₂ + 0.001 and TiO₂ + 0 discs. Empty wells on the microplates (Tissue Culture Polystyrene, TCPS) were also seeded to be used as the gold standard of the cell culture. Cells were cultured up to 21 days in a humidified atmosphere with 5 % CO₂ at 37 °C. To induce the differentiation to osteoblasts 2-phospho-L-ascorbic acid trisodium salt (2 mM, Sigma 49752), β-glycerophosphate disodium salt hydrate (10 mM, Sigma G9422) and dexamethasone (10⁻⁵ M, Sigma D4902, ≥97 %) were added to the supplemented MEM-alpha. Culture medium was renewed every 2–3 days.

Cell morphology was analyzed by SEM (Philips XL30) after 7 and 21 days. After each incubation time, cells were fixed with 2.5 % glutaraldehyde solution in PBS (Lonza BE17-512F) for 2 h at 4 °C. Samples were then washed three times for 30 min with PBS and dehydrated in graded acetone solutions (30 %, 50 %, 70 %, 80 %, 95 %) for 30 minutes in each solution and in absolute acetone for 1 h. After dehydration, samples were submitted to critical

1
2
3 point in CO₂, at 75 atm and 31.3 °C, mounted on metal stubs and sputter-coated with gold prior
4
5 to their analysis using a Philips XL30 scanning electron microscope (CACTI, University of
6
7 Vigo).

8
9 Cell proliferation was quantified after 7 and 21 days with the Cell Proliferation Kit I (MTT
10
11 assay, Roche), as described above. The plate was then incubated overnight and, after removing
12
13 the discs, the resulting colored solution was quantified at 595 and 655 nm using a Bio-Rad
14
15 Model 550 microplate spectrophotometer. Four replicates per material per condition were
16
17 evaluated and the complete experiment was repeated twice. TiO₂ discs without cell seeding
18
19 were also incubated as blanks.
20
21

22
23 Osteogenic activity was evaluated by quantifying the activity of the enzyme alkaline
24
25 phosphatase (ALP) after 7 and 21 days of incubation. After each incubation time, discs were
26
27 carefully rinsed twice with PBS and immersed in water. The cell lysates were obtained after the
28
29 osmotic shock followed by a thermal shock by transferring the lysates from 37 to -80 °C. ALP
30
31 activity was measured using a p-nitrophenol assay. Briefly, p-nitrophenyl phosphate, which is
32
33 colorless, was hydrolyzed by alkaline phosphatase at pH 10.5 and 37 °C to form free p-
34
35 nitrophenol, which is yellow. The reaction was stopped by adding NaOH and the absorbance
36
37 read at 405 nm in a microplate reader (Bio-Tek, USA). The kit (Alkaline Phosphatase Assay
38
39 Kit, Abcam) provides with ALP standards to calibrate the results and obtain the corresponding
40
41 concentrations of enzyme (U/mL) from the absorbance data. Both cell proliferation and
42
43 osteogenic activity protocols were also applied to the TCPS controls, as the gold standard
44
45 reference. Four replicates were used per material per condition and the complete experiments
46
47 were repeated twice. Discs without cell seeding were also incubated as blanks.
48
49
50

51 52 *2.5 Statistical analysis*

53
54 Data are presented as mean ± mean standard deviation (typical error) in error bars (n=4).
55
56 Differences between groups were analyzed according to Student's t-test with p<0.01 and p<0.05
57
58 considered statistically significant (99 % and 95 % of cases, respectively).
59
60

3. Results

3.1 Mesoporous thin films characterization and simvastatin loading

Mesoporous titania thin films were fabricated on glass disks by spin coating following the EISA procedure (Crepaldi *et al* 2003). An amphiphilic block-copolymer (Pluronic F127) was employed as pore template and TiCl_4 was used as TiO_2 precursor, both dissolved in ethanol. The controlled evaporation of the solvent led to assembly of the Pluronic F127 into micelles and the condensation of the precursor, generating an ordered mesophase. Stiffening of the inorganic network and removal of the template required a thermal treatment and ethanol extraction. Figure 1 shows scanning and transmission electron micrographs of the obtained thin films. Highly ordered pores forming a 3D cubic arrangement compatible with the $\text{Im}3\text{m}$ space group (body centered cubic order, commonly obtained when using Pluronic F127 as a template (Crepaldi *et al* 2003)) were observed. The interpore distance (from center to center of neighboring pores) for these mesoporous films was of 12 ± 2 nm, as determined from TEM and SEM image analysis. This value is in accordance with previously reported results (Crepaldi *et al* 2003). A film thickness of 95 ± 5 nm was measured from SEM cross section images (inset in figure 1(a)).

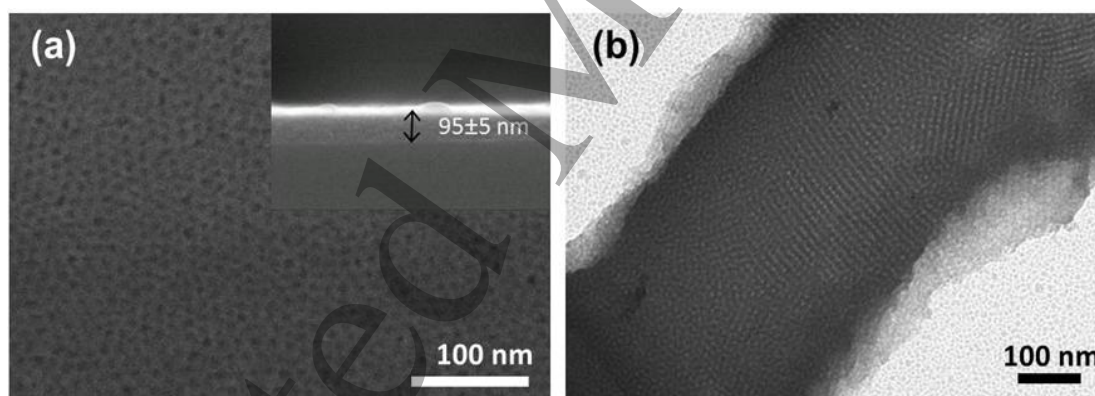
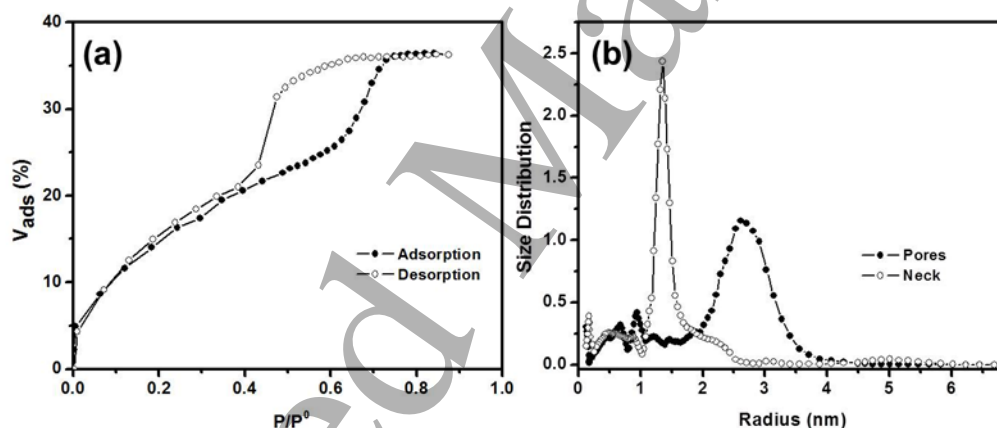


Figure 1. SEM (a) and TEM micrographs (b) of mesoporous titania thin films deposited on a glass disc. In (a) the inset is an image of the cross section of the same mesoporous thin film.

The removal of Pluronic F127 upon ethanol extraction (see experimental part for details) was evaluated by FTIR analysis and confirmed by the absence of the strong IR signals at around $2850\text{-}2930\text{ cm}^{-1}$ assigned to the C-H stretching vibration of the template (figure S1(a) in supporting material) (Socrates *et al* 2004). The crystalline structure of TiO_2 was evaluated by Raman spectroscopy, which revealed the characteristic lines of anatase TiO_2 phase at 150 (Eg),

1
2
3 194, 400 (B1g), and 636 (Eg) cm^{-1} (figure S1(b) in supporting material) (Wang *et al* 2013).
4
5 However, broad of peaks at 400 and 636 cm^{-1} indicates that the titania walls present a low
6 degree of crystalline order, in agreement with previous results (Angelomé PC *et al* 2007).
7
8 Finally, the accessible porosity and the pore size distribution of the mesoporous thin films were
9 evaluated by Environmental Ellipsometric Porosimetry (figure 2). The adsorption-desorption
10 isotherms shown in figure 2(a) are characteristic of mesoporous materials and demonstrate that
11 the accessible porosity of the obtained titania mesoporous thin film was around 36 %. The pore
12 size distribution plotted in figure 2(b) corresponds to pores of 5.5 nm (obtained from the
13 adsorption branch) and necks between the pores of 2.8 nm (obtained from desorption branch).
14
15 The porosity and pore sizes are again in agreement with previous results obtained for calcined
16 mesoporous films (Violi *et al* 2012), which confirms the efficiency of the extraction approach to
17 eliminate the template.
18
19
20
21
22
23
24
25
26
27
28
29
30



31
32
33
34
35
36
37
38
39
40
41
42
43
44
45
46 Figure 2. Water adsorption-desorption isotherms for a mesoporous titania thin film (a). Pore size
47 (solid circles) and neck size (empty circle) distributions obtained from adsorption-desorption
48 branches of isotherms through the Kelvin equation (b).
49
50
51
52

53 The high porosity of the mesoporous titania thin films together with their bioactive properties
54 motivated us to load the mesostructures with simvastatin. Importantly, simvastatin is a molecule
55 (see figure S2 in supporting information) with dimensions smaller than the mesoporous pore
56 and neck sizes. In addition, the molecule presents ester and hydroxyl groups, which are known
57 to be complexing agents for mesoporous TiO_2 (Angelomé and Soler-Illia 2005). The ability of
58
59
60

simvastatin to diffuse within the mesoporous thin film and attach to the TiO_2 walls was confirmed by FTIR spectroscopy. As shown in figure 3, the FTIR spectrum of a titania thin film loaded with 5 g/L of simvastatin displays the characteristic FTIR signals of this molecule, including symmetric and asymmetric stretching vibration of C–H ($2800\text{--}3000\text{ cm}^{-1}$ and 1456 cm^{-1}), ester carbonyl C=O stretch (1695 cm^{-1}) and bending of both C–O–C lactone (1265 cm^{-1}) and ester (1161 cm^{-1}) (Ledeti *et al* 2015), together with the ν_{TiOTi} vibrations of the oxide.

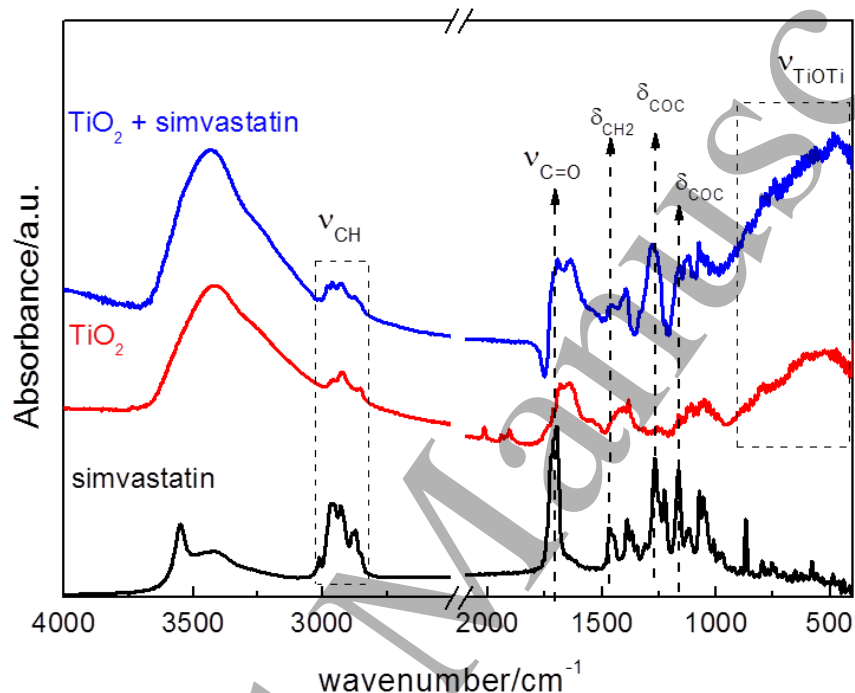


Figure 3. FTIR spectra of simvastatin (black), a mesoporous titania thin film (red) and a mesoporous titania thin film loaded with simvastatin (blue).

3.2 Biological response of simvastatin-loaded mesoporous thin films

Figure 4 presents the direct evaluation of MC3T3-E1 pre-osteoblasts viability with a wide range of simvastatin concentrations from 0 g/L to 5 g/L, in the growth media. The samples with 0 g/L were considered as the positive control for optimal cell viability. After 4 days of incubation, simvastatin concentrations $\leq 0.01\text{ g/L}$ promoted cell viability within the same range as the 0 g/L (for 0.01 g/L) or statistically significantly higher ($p < 0.01$) (for 0.001 g/L) than both 0 g/L and 0.01 g/L concentrations. However, higher simvastatin concentrations $\geq 0.1\text{ g/L}$ (from 0.1 to 5 g/L) were found to promote low cell viability, with optical density values below 0.4 which is

considered as a cytotoxic level, and significantly lower cell viability ($p < 0.01$) than the positive control (0 g/L) for all cases. The 0.05 g/L samples promoted higher cell viability (> 0.4), but still statistically significantly lower ($p < 0.01$) than the positive control. Therefore, taking into account these results, the cytotoxicity threshold for simvastatin with MC3T3-E1 pre-osteoblasts could be established on simvastatin concentrations ≥ 0.05 g/L. Moreover 0.01 g/L and 0.001 g/L were considered as the optimal simvastatin concentrations to be loaded within the mesoporous titania thin films, as they seemed to ensure the same levels of cell viability or higher (in case of 0.001 g/L) than the growth medium (without simvastatin).

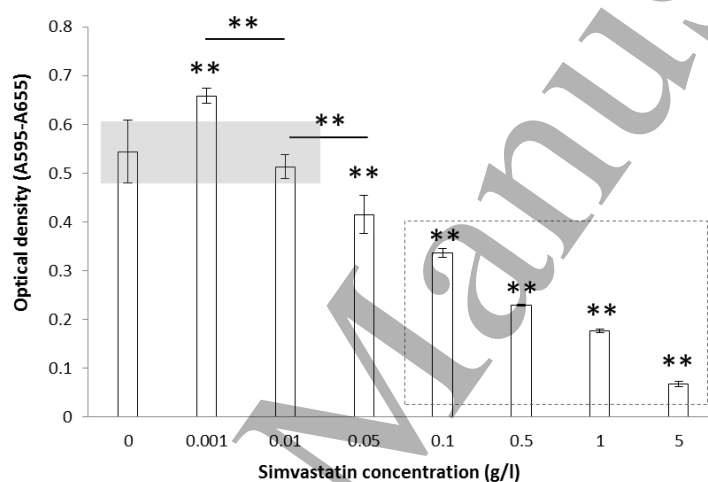
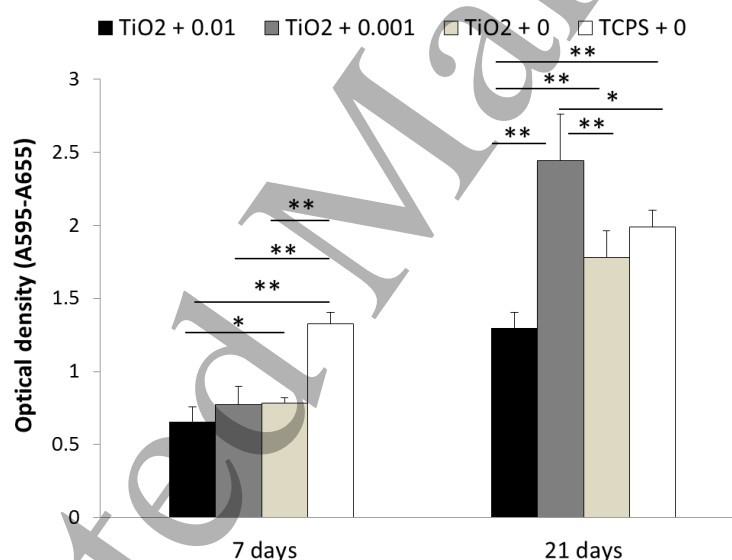


Figure 4. MC3T3-E1 pre-osteoblasts viability after 4 days of incubation with different concentrations (g/L) of simvastatin in supplemented MEM-alpha growth medium. Significant statistical differences are presented as ** for $p < 0.01$ (99%) and * for $p < 0.05$ (95%).

TiO₂ thin films were then loaded with the two optimal simvastatin concentrations of 0.01 g/L and 0.001 g/L and incubated with MC3T3-E1 pre-osteoblasts to evaluate their proliferation and osteogenic activity. MC3T3-E1 pre-osteoblasts proliferation on the loaded thin film coatings together with the experimental controls (0 g/L and TCPS) is presented in figure 5, as a function of incubation time (7 and 21 days). Cell proliferation on the three tested mesoporous titania thin films was significantly lower ($p < 0.01$) than on the TCPS after 7 days of incubation, where the optical density value above 1.0 at this latter validated the healthy stage of the cells. After 21

1
2
3 days of incubation, no statistical differences were found between cell proliferation at 0 g/L
4
5 mesoporous titania thin films and TCPS, thereby validating the biocompatibility of the films
6
7 together with their proper sterilization and the optimal evaporation of ethanol during the loading
8
9 procedure (as these 0 g/L samples were subjected to the same process as the loaded ones).
10
11 Moreover, cell proliferation increased for all tested conditions, as compared to each value at 7
12
13 days. In more detail, cell proliferation at 0.01 g/L was significantly lower ($p < 0.01$) than on
14
15 0.001 g/L and 0 g/L mesoporous thin films. On the other hand, the 0.001 g/L films promoted
16
17 significantly higher cell proliferation than the 0.01 g/L ($p < 0.01$) and the 0 g/L ($p < 0.01$) films.
18
19 We therefore conclude that, loading of mesoporous titania thin films with 0.001g/L simvastatin
20
21 significantly promoted the proliferation of MC3T3-E1 pre-osteoblasts after 21 days of
22
23 incubation, while the cell proliferation rate in case of 0.01 g/L loading was significantly slowed
24
25 down.
26
27
28

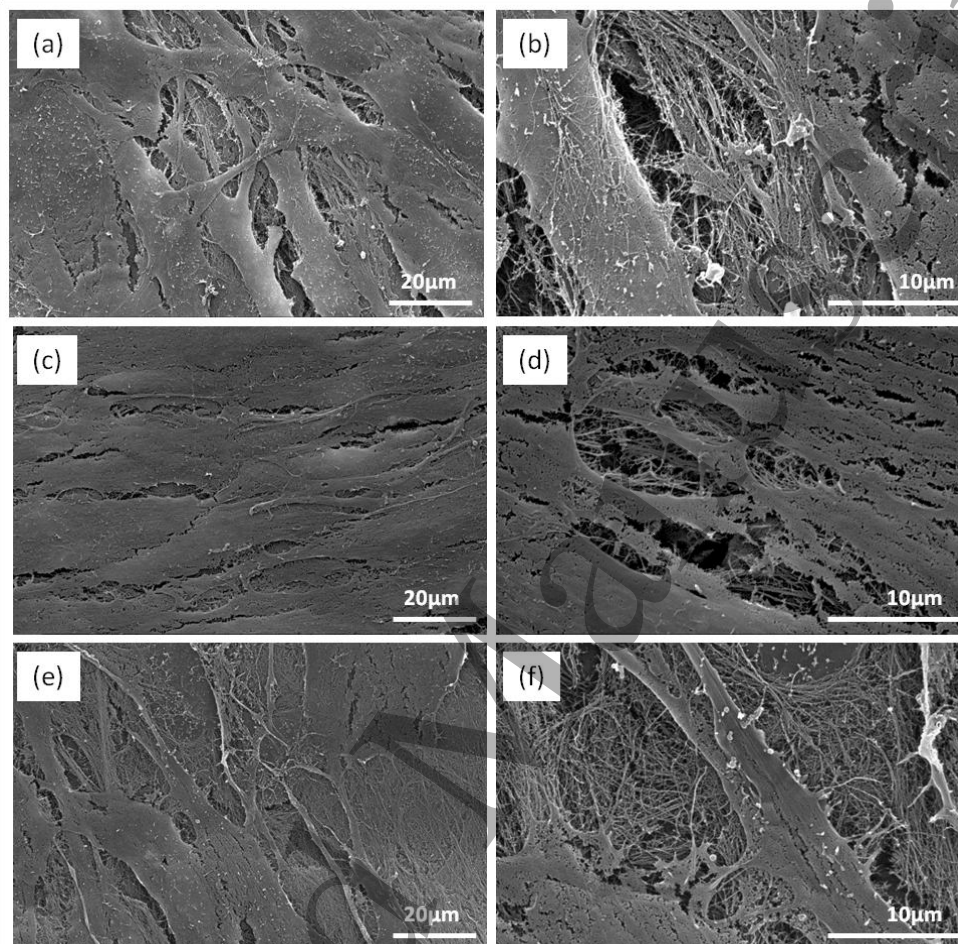


29
30
31
32
33
34
35
36
37
38
39
40
41
42
43
44
45
46
47
48
49
50
51
52
53
54
55
56
57
58
59
60

Figure 5. MC3T3-E1 pre-osteoblasts proliferation on mesoporous titania thin films loaded with 0.01 g/L, 0.001 g/L and 0 g/L of simvastatin up to 21 days of incubation. Cell proliferation for tissue culture polystyrene (TCPS) is also presented.

The effect of simvastatin loaded titania thin films on cell morphology after 21 days of incubation was analyzed by SEM. Figure 6 shows SEM micrographs of MC3T3-E1 pre-osteoblasts monolayers on thin films loaded with simvastatin at the 0.01 g/L (a, b), 0.001 g/L (c,

1
2
3 d) and 0 g/L (e, f). It is important to note that a cell monolayer covering the whole film surface
4 was observed in all cases (figure 6a,c,e). Meanwhile, formation of complex filament networks
5 and synthesis of pre-mineralized matrix were evident in 0.01 g/L (figure 6(b)) and 0 g/L (figure
6 6 (f)) thin films, and less intense in the case of 0.001g/L (figure 6(d)).
7
8
9
10
11



12
13
14
15
16
17
18
19
20
21
22
23
24
25
26
27
28
29
30
31
32
33
34
35
36
37
38
39
40
41
42
43
44
45
46
47
48
49
50
51
52
53
54
55
56
57
58
59
60
Figure 6. SEM micrographs of MC3T3-E1 pre-osteoblasts morphology on 0.01 g/L (a,b), 0.001 g/L(c,d) and 0 g/L (e,f) simvastatin loaded mesoporous titania thin films after 21 days of incubation.

The osteogenic activity of the MC3T3-E1 pre-osteoblasts was evaluated by quantifying the synthesis of the early marker alkaline phosphatase (ALP enzyme) after 7 and 21 days (figure 7). Thus, the dramatic and expected increase at the ALP synthesis by the cells at 21 days of incubation on the TCPS, compared to the value quantified at 7 days, validated the healthy stage of the cells and, therefore, the experiment. Focusing on the titania thin films, the absence of

ALP synthesis was observed at 7 days of incubation, being significantly lower ($p < 0.01$) than in TCPS. A dramatic increase of ALP synthesis was also detected for the three tested titania thin films at 21 days of incubation, in analogy to TCPS, which proved the differentiation of the MC3T3-E1 pre-osteoblast like cells into osteoblasts. However differences were found between them, with significantly higher values for 0.01 g/L of simvastatin than for the two other films with lower concentrations: 0.001 ($p < 0.05$) and 0 g/L ($p < 0.01$). These two lower concentrations presented also significantly lower ALP synthesis than the TCPS ($p < 0.05$ and $p < 0.01$, respectively), while the 0.01 promoted the osteogenic activity at the same level than the gold standard.

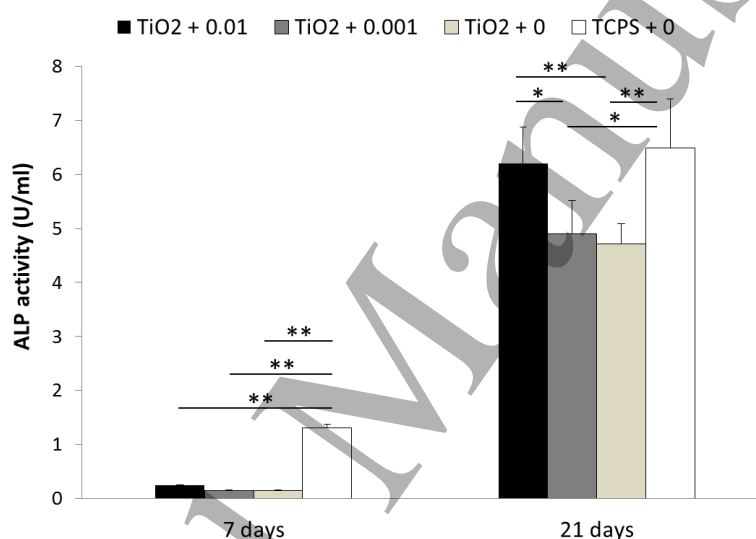


Figure 7. MC3T3-E1 pre-osteoblasts osteogenic activity (ALP synthesis) on mesoporous titania thin films loaded with 0.01 g/L, 0.001 g/L and 0 g/L of simvastatin up to 21 days of incubation. ALP synthesis quantified on the tissue culture polystyrene (TCPS) is also presented.

In figure 8 the SEM analysis of the cell monolayer microstructure at 21 days of incubation on the 0.01g/L thin films is presented. At this time of incubation, cells are found to spread on a flat morphology (figure 8(a)) with abundant lamellipodia to establish cell to cell contacts covering the entire surface and growing directly over cell layer (figure 8(b)), being the thin film under the thick layer of cells. The synthesis of pre-mineralized extracellular matrix can be observed with the formation of a complex network of pre-collagen filaments (figure 8c,d).

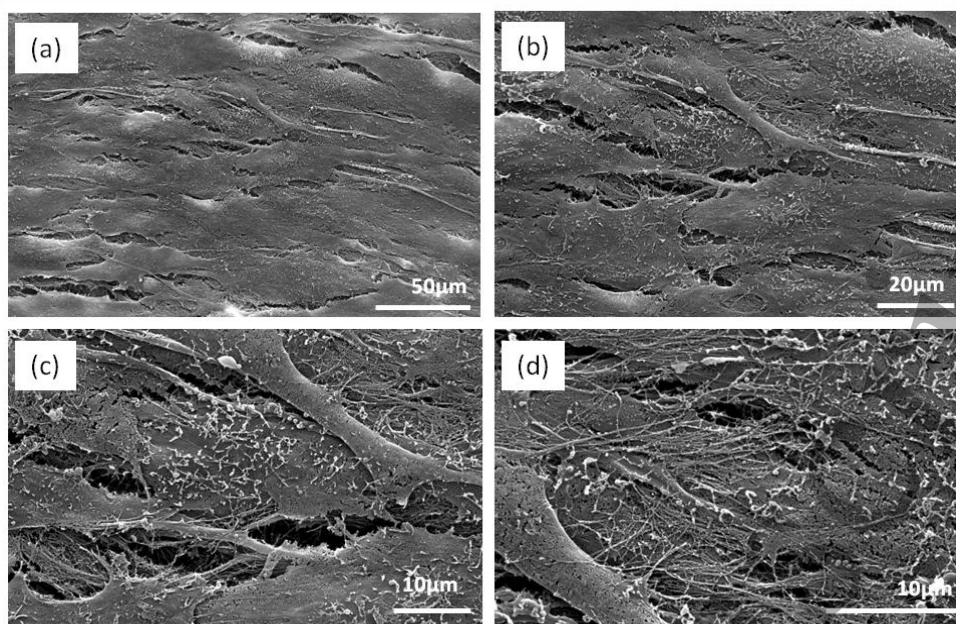


Figure 8. SEM micrographs of MC3T3-E1 pre-osteoblasts morphology on mesoporous titania thin films loaded with 0.01 g/L of simvastatin after 21 days of incubation.

4. Discussion

In the present work, the promotion of osteogenic activity by simvastatin upon loading in mesoporous titania thin films was evaluated on MC3T3-E1 pre-osteoblasts, along with the cytotoxicity threshold.

In detail, simvastatin loading within mesoporous titania thin films was confirmed together with the physicochemical characterization of the films. The abundance of highly ordered pores forming a 3D cubic arrangement was proved on the mesoporous thin films of TiO_2 , with an interpore distance of 12 ± 2 nm and a layer thickness of 95 ± 5 nm, as presented in figure 1. The accessible porosity was quantified (figure 2) to be 36 %, with pore diameters of 5.5 nm and necks between the pores of 2.8 nm. These data, together with the simvastatin dimensions (1.2 nm x 1.2 nm) ensure the ability of the molecule to diffuse within the pores and attach to the titania walls, through ester and hydroxyl groups. Simvastatin loading was confirmed by FTIR spectroscopy (figure 3) where $\nu_{\text{C=O}}$, ν_{CH} and ν_{COC} vibrations were detected, together with ν_{TiOTi} vibrations assigned to the mesoporous film. An enhanced osteointegration was previously

1
2
3 observed for mesoporous titania with 6 nm of pore diameter (Harmankaya *et al* 2013, Galli *et al*
4
5 2014, Karlsson *et al* 2015b).

6
7 The ability of mesoporous titania to form chemical bonds with apatite through Ca^{2+} cations
8
9 (Karlsson *et al* 2014), in combination with its suitability as drug delivery system, render it
10
11 unique properties when used as implant coatings. The loading of different bone formation
12
13 promoters in mesoporous titania films (alendronate (Karlsson *et al* 2015b), raloxifene
14
15 (Harmankaya *et al* 2013) or magnesium (Galli *et al* 2014)) has been reported. In this context,
16
17 the loading and osteogenic activity promoted by simvastatin are of interest, as it is currently
18
19 prescribed to inhibit cholesterol biosynthesis and already proven as a promoter of osteogenic
20
21 differentiation (Maeda *et al* 2001).
22
23

24
25 When simvastatin was directly added to the cells in growth media (figure 4) promoted MC3T3-
26
27 E1 pre-osteoblasts viability at concentrations ≤ 0.01 g/L, but inhibited viability at higher
28
29 concentrations ≥ 0.1 g/L, with a cytotoxicity threshold at 0.05 g/L. This viability trend was
30
31 maintained upon simvastatin loading into mesoporous titania thin films. Indeed, concentrations
32
33 of 0.01 g/L and 0.001 g/L of simvastatin promoted the MC3T3-E1 proliferation, being
34
35 statistically higher for 0.001 g/L (figures 5 and 6), and the osteogenic activity, being statistically
36
37 higher for 0.01 g/L (figures 7 and 8) after 21 days of incubation. Maeda *et al* (2001) proved
38
39 higher levels of osteoblast differentiation and mineralization when 10^{-7} M simvastatin was
40
41 directly added to MC3T3-E1, as compared to 10^{-8} and 10^{-9} M. In our work the highest osteoblast
42
43 differentiation was achieved for 0.001 g/L (2.4×10^{-6} M) and 0.01 g/L (2.4×10^{-5} M) upon loading
44
45 in the thin films. Moreover, the cytotoxicity threshold obtained when cells were directly
46
47 incubated with simvastatin was established as 0.05 g/L (1.2×10^{-4} M). These results demonstrate
48
49 that there was still margin *in vitro* to enrich with higher concentrations of simvastatin for this
50
51 cell line.
52
53

54
55 It is important to note that despite the concentrations of statins in the bone marrow have not
56
57 been well established yet, it is accepted that osteoblasts and osteoclasts may be exposed to very
58
59 low concentrations (Kheirallah and Almeshaly 2016). In fact, within the strategy of local
60
administration, the coating of a porous and well interconnected scaffold of TiO_2 with alginate

1
2
3 hydrogel containing 10 nM of simvastatin was reported to promote the osteogenic
4 differentiation of human mesenchymal stem cells (Pullisaar *et al* 2014). The presence of
5 alginate and the entire scaffold of titania (8 mm in height and 9 mm in diameter) have surely
6 contributed to these good results for such a low dose of simvastatin, against the thin film titania
7 coatings (95 nm in height and 6mm in diameter) used at the present work.

8
9
10
11
12
13
14 On the other hand, higher concentrations of simvastatin were also successfully evaluated in
15 tibial defect of rabbit model in terms of osteointegration, bone ingrowth and neovascularization.
16
17 Thus, Liu *et al* (2016) evaluated porous titanium alloy scaffolds (5 mm diameter and 6 mm
18 thickness) filled with simvastatin/poloxamer 407 hydrogel with final simvastatin concentrations
19 of 0.1 g/L and 0.5 g/L. A significantly increased cortical bone was quantified with the 0.5 g/L
20 simvastatin group (0.5 mg), being nearly identical to that of normal cortical bone at 8 weeks.
21
22

23
24
25
26
27 Moreover, in a recent review about the simvastatin influence on animal model studies (Sendyk
28 *et al* 2016 the difficulty to equalize the optimal range of doses/concentrations of this drug was
29 discussed. Successful results were found for simvastatin doses which range from 10^{-4} to 10^{-7} M,
30 when directly applied on titanium implants' surfaces or in calcium phosphate coatings, and from
31 50 μ g to 10 mg on oxidized surface of implants, combined with chitosan as a coating or directly
32 injected in to the femurs. However, topical application has been shown to cause local
33 inflammation in high doses (Sendyk *et al* 2016). There is, therefore, a lack of consensus in the
34 literature in relation to the effective doses of simvastatin, even when being tested alone directly
35 with cells, without any carrier. Moreover, it seems to strongly depend on the drug release
36 patterns from the loading material or administration strategy used.
37
38
39
40
41
42
43
44
45
46
47

48 49 **5. Conclusions**

50
51 The ability of simvastatin to be loaded in mesoporous titania thin films was demonstrated
52 together with its effectiveness in terms of pro-osteogenic activity. In detail, 36 % of accessible
53 porosity with pore diameters of 5.5 nm interpore distances of 12 ± 2 nm in TiO₂ thin films with
54 thicknesses of 95 ± 5 nm, were proven to favor the diffusion of simvastatin within the pores and
55 its attachment to the titania walls through ester and hydroxyl groups. Simvastatin concentrations
56
57
58
59
60 ≤ 0.01 g/L were proven to promote MC3T3-E1 pre-osteoblasts viability, while concentrations \geq

1
2
3 0.1 g/L inhibited it, being the cytotoxicity threshold established as 0.05 g/L. Finally, a
4
5 concentration of 0.001 g/L of simvastatin upon loaded on the mesoporous titania thin films
6
7 promoted statistically higher MC3T3-E1 proliferation and a concentration of 0.01 g/L
8
9 statistically higher osteogenic activity after 21 days in comparison to unloaded films. The *in*
10
11 *vitro* effectiveness of simvastatin loading in mesoporous titania thin films was demonstrated,
12
13 with potential application in the field of bone regeneration, especially when an implant is
14
15 required. This work opens the possibility of using TiO₂ mesoporous thin films as carriers for
16
17 local delivery of simvastatin to coat metallic prosthesis and provide them with pro-osteogenic
18
19 activity and better osteointegration. Deep evaluation on the release pattern of this molecule is
20
21 required as well as the performance *in vivo* of metallic implants coated with these simvastatin-
22
23 loaded TiO₂ thin films.
24
25

26 27 28 **Acknowledgements**

29
30 This work was partially funded by Xunta de Galicia GRC2013-008 and by the Ministerio de
31
32 Economía y Competitividad (MINECO, Grant MAT2016-77809-R). M. López-Álvarez and V.
33
34 López-Puente thank funding from FP7/REFPOT-2012-2013.1 (n-316265) BIOCAPS and
35
36 Spanish MINECO FPI scholarship, respectively. PCA acknowledges the financial support of
37
38 ANPCyT (PICT 2012-0111) Technical staff of CACTI (University of Vigo) is gratefully
39
40 acknowledged.
41
42

43 44 **References**

45
46 Allon N, Saxena A, Chambers C and Doctor BP 2012 A new liposome-based gene delivery
47
48 system targeting lung epithelial cells using endothelin antagonist *J Control Release* **160**
49
50 217-24
51
52 Angelomé PC, Andrini L, Calvo ME, Requejo FG, Bilmes SA and Soler-Illia GJAA 2007
53
54 Mesoporous anatase TiO₂ films: use of Ti K XANES for the quantification of the
55
56 nano-crystalline character and substrate effects in the photocatalysis behavior *J Phys*
57
58 *Chem C* **11** 10886-93
59
60

- 1
2
3 Angelomé PC and Soler-Illia GJAA 2005 Organically modified transition-metal oxide
4 mesoporous thin films and xerogels *Chem Mater* **17** 322-31
5
6
7 Bellino MG, Golbert S, de Marzi MC, Soler-Illia GJAA and Desimone MF 2013 Controlled
8 adhesion and proliferation of a human osteoblastic cell line by tuning the nanoporosity of
9 titania and silica coatings *Biomater Sci* **1** 186-9
10
11
12 Boissiere C, Grosso D, Lepoutre S, Nicole L, Bruneau AB and Sanchez C 2005 Porosity and
13 mechanical properties of mesoporous thin films assessed by environmental ellipsometric
14 porosimetry *Langmuir* **21** 12362-71
15
16
17 Brinker CJ, Lu Y, Sellinger A and Fan H 1999 Evaporation-induced self-assembly:
18 nanostructures made easy *Adv Mater* **11** 579-85
19
20
21 Crepaldi EL, Soler-Illia GJAA, Grosso D, Cagnol F, Ribot F and Sanchez C 2003 Controlled
22 formation of highly organized mesoporous titania thin films: from mesostructured hybrids
23 to mesoporous nanoanatase TiO₂ *J Am Chem Soc* **125** 9770-86
24
25
26 Galli S, Naito Y, Karlsson J, He W, Miyamoto I, Xue Y, Andersson M, Mustafa K, Wennerberg
27 A and Jimbo R 2014 Local release of magnesium from mesoporous TiO₂ coatings
28 stimulates the peri-implant expression of osteogenic markers and improves
29 osteoconductivity *in vivo Acta Biomater* **10** 5193-201
30
31
32 Gertler G, Fleminger G and Rapaport H 2010 Characterizing the adsorption of peptides to TiO₂
33 in aqueous solutions by liquid chromatography *Langmuir* **26** 6457-63
34
35
36 Harmankaya N, Karlsson J, Palmquist A, Halvarsson M, Igawa K, Andersson M and Tengvall P
37 2013 Raloxifene and alendronate containing thin mesoporous titanium oxide films
38 improve implant fixation to bone *Acta Biomater* **9** 7064-73
39
40
41 Kanis JA, McCloskey EV, Johansson H, Cooper C, Rizzoli R and Reginster JY 2013 European
42 guidance for the diagnosis and management of osteoporosis in postmenopausal women
43
44
45 *Osteoporos Int* **24** 23-57
46
47
48 Karlsson J, Sundell G, Thuvander M and Andersson M 2014 Atomically resolved tissue
49 integration *Nano Lett* **14** 4220-3
50
51
52
53
54
55
56
57
58
59
60

- 1
2
3 Karlsson J, Atefyekta S and Andersson M 2015a Controlling drug delivery kinetics from
4
5 mesoporous titania thin films by pore size and surface energy *Int J Nanomedicine* **10**
6
7 4425-36
8
9
10 Karlsson J, Harmankaya N, Allard S, Palmquist A, Halvarsson M, Tengvall P and Andersson M
11
12 2015b *Ex vivo* alendronate localization at the mesoporous titania implant/bone interface *J*
13
14 *Mater Sci Mater Med* **26** 1-8
15
16 Kheirallah M and Almeshaly H 2016 Simvastatin, dosage and delivery system for supporting
17
18 bone regeneration, an update review *J Oral Maxillofac Surg Med Pathol* **28** 205-9
19
20
21 Ledeti I, Vlase G, Vlase T, Suta LM, Todea A and Fuias A 2015 Selection of solid-state
22
23 excipients for simvastatin dosage forms through thermal and nonthermal techniques *J*
24
25 *Therm Anal Calorim* **121** 1093-102
26
27 Liu H, Li W, Liu C, Tan J, Wang H, Hai B, Cai H, Leng HJ, Liu ZJ and Song CL 2016
28
29 Incorporating simvastatin/poloxamer 407 hydrogel into 3D-printed porous Ti6Al4V
30
31 scaffolds for the promotion of angiogenesis, osseointegration and bone ingrowth
32
33 *Biofabrication* **8** 045012
34
35
36 Maeda T, Matsunuma A, Kawane T and Horiuchi N 2001 Simvastatin promotes osteoblast
37
38 differentiation and mineralization in MC3T3-E1 cells *Biochem Biophys Res Commun* **280**
39
40 874-7
41
42
43 McMaster WA, Wang X and Caruso RA 2012 Collagen-templated bioactive titanium dioxide
44
45 porous networks for drug delivery *ACS Appl Mater Interfaces* **4** 4717-25
46
47
48 Meretoja VV, Tirri T, Aaritalo V, Walboomers XF, Jansen JA and Narhi TO 2007 Titania and
49
50 titania-silica coatings for titanium: Comparison of ectopic bone formation within cell-
51
52 seeded scaffolds *Tissue Eng* **13** 855-63
53
54
55 Mundy G, Garrett R, Harris S, Chan J, Chen D, Rossini G, Boyce B, Zhao M and Gutierrez G
56
57 1999 Stimulation of bone formation *in vitro* and in rodents by statins *Science* **286** 1946-9
58
59
60 Pullisaar H, Reseland JE, Haugen HJ, Brinchmann JE and Ostrup E 2014 Simvastatin coating of
TiO₂ scaffold induces osteogenic differentiation of human adipose tissue-derived
mesenchymal stem cells *Biochem Biophys Res Commun* **447** 139-44

- 1
2
3 Sanchez C, Boissiere C, Grosso D, Laberty C and Nicole L 2008 Design, synthesis, and
4
5 properties of inorganic and hybrid thin films having periodically organized nanoporosity
6
7
8 *Chem Mater* **20** 682-737
- 9
10 Sayar F, Fallah S, Akhondi N and Jamshidi S 2016 Association of serum lipid indices and statin
11
12 consumption with periodontal status *Oral Dis* **22** 775-80
- 13
14 Sendik DI, Deboni MCZ, Pannuti CM, Naclerio-Homem MG, Wennerberg A 2016 The
15
16 influence of statins on osseointegration: a systematic review of animal model studies *J*
17
18 *Oral Rehabil* **43** 873-882
- 19
20 Socrates G 2004 Infrared and Raman characteristic group frequencies: Tables and charts, 3er
21
22 edition New York Wiley ISBN: 978-0-470-09307-8
- 23
24 Soler-Illia GJAA, Angelomé PC, Fuertes MC, Grosso D and Boissiere C 2012 Critical aspects
25
26 in the production of periodically ordered mesoporous titania thin films *Nanoscale* **4** 2549-
27
28 66
- 29
30
31 Violi IL, Perez MD, Fuertes MC and Soler-Illia GJAA 2012 Highly ordered accessible and
32
33 nanocrystalline mesoporous TiO₂ thin films on transparent conductive substrates *ACS*
34
35 *Appl Mater Interfaces* **4** 4320-30
- 36
37
38 Wang X, Wu G, Zhou B and Shen J 2013 Optical constants of crystallized TiO₂ coatings
39
40 prepared by sol-gel process *Materials* **6** 2819-30
- 41
42 Xia W, Grandfield K, Hoess A, Ballo A, Cai Y and Engqvist H 2012 Mesoporous titanium
43
44 dioxide coating for metallic implants *J Biomed Mater Res Part B* **100B** 82-93
- 45
46 Yin H, Shi ZG, Yu YS, Hu J, Wang R, Luan ZP and Guo DH 2012 Protection against
47
48 osteoporosis by statins is linked to a reduction of oxidative stress and restoration of nitric
49
50 oxide formation in aged and ovariectomized rats *Eur J Pharmacol* **674** 200-6
- 51
52
53
54
55
56
57
58
59
60